The application of disturbance observer-based sliding mode control for magnetic levitation systems

Z G Sun[1], **N C Cheung**[1*], **S W Zhao**[1], and **W C Gan**[2]
[1]Department of Electrical Engineering, Hong Kong Polytechnic University, Kowloon, Hong Kong
[2]R&D Motion, ASM Assembly Automation Ltd., Kwai Chung, N.T., Hong Kong

The manuscript was received on 16 February 2009 and was accepted after revision for publication on 9 November 2009.

DOI: 10.1243/09544062JMES1572

Abstract: A control algorithm for the position tracking of a magnetic levitation system is presented in this article. The magnetic levitation system is well known for its non-linear dynamic characteristics and open-loop instability. The external disturbances will deteriorate the dynamic performance of the magnetic levitation system, and may give rise to system instability. This problem triggers enormous interests in designing various controllers for the non-linear dynamic system. In this article, a magnetic levitation system is first modelled. Then, a sliding mode controller is proposed, with a simple yet effective disturbance observer to perform disturbance rejection. Both the simulation results and the experimental results verify the validity of the robust controller.

Keywords: magnetic levitation system, non-linear dynamic characteristics, sliding mode control, disturbance observer, real-time implementation

1 INTRODUCTION

In recent years, magnetic levitation issues have attracted many scientists and engineers' attention owing to its friction-free dynamic motions. A magnetic levitated metallic ball system has been a subject of considerable interest to illustrate many fundamental principles of electrical and electronic engineering, such as electromagnetics, circuit design, and control algorithms. The magnetic levitation system is non-linear in nature and is unstable in open loop. The system performance would be heavily affected by various disturbances. These challenging characteristics stimulate the design of various controllers in order to improve the system performances.

A magnetic suspension system was designed in reference [**1**], and the proportional plus derivative (PD) control was adopted to levitate the metallic ball, but the detailed system performances of the magnetic suspension system were not analytically examined. Feedback linearization control of the magnetic levitation system has been applied by numerous researchers because of the inherent non-linearities of the system [**2**, **3**]. The findings in reference [**2**] revealed that the feedback linearization method were superior to the classical proportional-integral-derivative (PID) control in a large air gap of the magnetic levitation system; however, the disturbance of the system was not taken into account. While the disturbance was considered in reference [**3**], the experimental results indicated that there were static errors due to the magnetic levitation mass perturbation. In reference [**4**], an adaptive non-linear control composed of the feedback linearization method was introduced, and the experimental results reflected its robustness to system parameters uncertainties. However, adaptive control is computationally intensive and time consuming; also, the disturbance was not taken into consideration.

Sliding mode control (SMC) is applied widely in electro-mechanical systems [**5**–**7**]. It is efficient in controlling complicated high-order dynamic plants operating under uncertainty conditions [**8**]. The SMC focuses on two domains: the selection of the sliding surface and the design of the sliding control law. The sliding surface will decide the desirable behaviour of the operating system. The sliding control law will force the system state trajectories towards the sliding surface and stay on it.

Owing to the above merits, the SMC is one of the effective candidates for the magnetic levitation

*Corresponding author: Department of Electrical Engineering, Hong Kong Polytechnic University, Kowloon, Hong Kong.
email: norbert.cheung@polyu.edu.hk

system. The purposes of references [**9**] and [**10**] were to replace the linear sliding surface with the nonlinear one; as a result, the desired performances of the magnetic levitation systems were improved. In reference [**11**], the sliding mode equivalence control with the exponential reaching law was adopted to a magnetic levitation system. Although the simulation results show that the response air gap could follow the command under the assumption of disturbances, there was no real-time implementation to prove the results.

For improving the system performance, some hybrid controllers including the SMC are applied on the magnetic levitation systems. For instance, the integral sliding mode controller with grey forecast was proposed in reference [**12**]; a combination of the SMC and radial basis function network was employed to design the controller in reference [**13**]. Although experimental results suggest the effectiveness of these methods, the algorithms are complicated and time consuming.

In this article, a simple yet effective disturbance observer (DO) is designed for the SMC of the magnetic levitation system. First, the model of the magnetic levitation system is built. Then, a sliding mode controller is designed based on the assumption of a known disturbance range. After investigating the closed-loop system performances, the discrepancy between the system dynamic characteristic and the static characteristic is revealed, that is, the higher the parameter gain to guarantee the zero steady error, the more the possibility that the system has poor dynamic performance, and vice versa. Hence, a simple DO is integrated into the controller in order to eliminate the effect of the disturbance. The simulation results show the availability of the controller. The last area of concern is that of validating the algorithms by real-time implementation, and the experimental results matched the simulation ones very well.

The organization of this article is as follows. The modelling of the magnetic levitation system is discussed in section 2. In section 3, the sliding mode controller and the DO are proposed and analysed for the magnetic levitation system. In section 4, the results of these controllers are simulated through Matlab and Simulink. The real-time implementations of the magnetic system are carried out to verify the proposed algorithms in section 5. Finally, the concluding remarks are given in section 6.

2 MODEL OF THE MAGNETIC LEVITATION SYSTEM

Figure 1 shows the experimental set-up of the magnetic levitation system, and the schematic diagram is given in Fig. 2. The experimental set-up is only an example for the magnetic levitation system, and the control method discussed later can be applied to any other typical magnetic levitation system. The magnetic levitation system is manufactured by Googol Technology Limited. The magnetic levitation system consists of an electromagnet, a steel ball, a light source, a position sensor, a data acquisition analog to digital/digital to analog (AD/DA) board, a control computer, and a drive circuit. The steel ball can be suspended at the desired set point by the electromagnetic force, which can be adjusted by the input current. The feedback apparatus includes light emitting diode (LED) light source and optoelectronic sensor. There is a slot in the light receiver panel to detect the light intensity, and it can be generated to relate voltage signals with the range from -10 to 0 V. The output photo-voltage signals from the optoelectronic sensor are transferred to the controller through the circuit's signal process and AD board data collection. By analysing those data, the controller regulates the input current to implement on the electromagnet to match the levitation requirements. The above is the basic operational principle of this magnetic levitation system, and the system model is considered as follows.

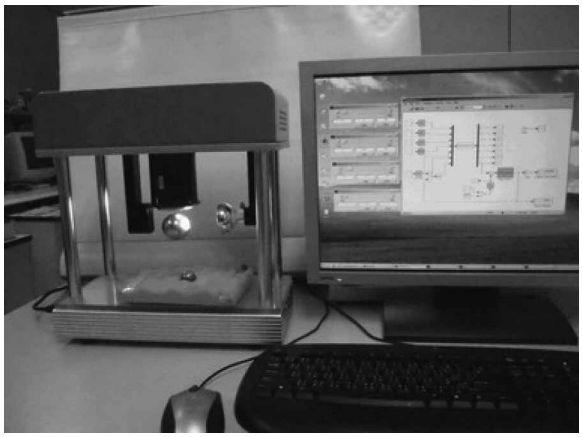

Fig. 1 Experimental set-up of the magnetic levitation system

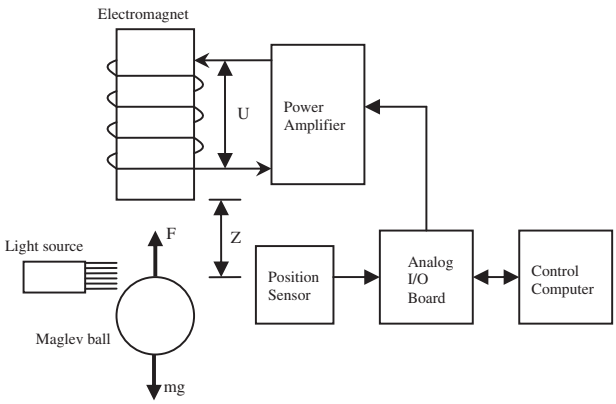

Fig. 2 Schematic diagram of the magnetic levitation system

2.1 Mathematic equations of model

The model of the magnetic levitation system can be divided into three parts: mechanical kinetics model, electromagnetic force model, and electrical model.

2.1.1 Mechanical kinetics model

The differential equation can be written as

$$m\frac{\mathrm{d}^2 z(t)}{\mathrm{d}t^2} = F(i,z) + mg \tag{1}$$

where m is the quality of the steel ball, z is the air gap distance between the electromagnet and steel ball, F is the electromagnetic force, i is the current, and g is the gravitational acceleration.

2.1.2 Electromagnetic force model

The electromagnetic co-energy W can be conducted from the virtual work

$$W(i,z) = \frac{1}{2}L(i,z)i^2 \tag{2}$$

where L denotes the inductance of the electromagnet coil and i denotes the current through the electromagnet.

The inductance L can be regarded as a function of z for this magnetic levitated ball system [**14**]

$$L = L_1 + \frac{L_0}{1 + z/p} \tag{3}$$

where $L_1 = L(\infty)$, $L_0 = L(0) - L(\infty)$, and p is the positive constant coefficient. $L(\infty)$ is the inductance when the ball is removed, whereas $L(0)$ is the inductance when the ball is in contact with the coil. The coefficients can be obtained from the experiment, which involves determining the minimum current required to levitate the steel ball at various positions [**15**, **16**].

Hence, the electromagnetic force can be written as

$$F(i,z) = \frac{\partial W(i,z)}{\partial z} = \frac{1}{2}\frac{\partial L}{\partial z}i^2 = -\frac{L_0 i^2}{2p(1+z/p)^2} \tag{4}$$

Equation (4) shows the non-linearity of the magnetic levitation system since the electromagnetic force is the non-linear function of the air gap distance and current.

2.1.3 Electrical model

The differential equation can be represented as follows

$$u(t) = R_c i(t) + \frac{\mathrm{d}\lambda(i,z)}{\mathrm{d}t} \tag{5}$$

where u denotes the terminal voltage on the electromagnet, R_c denotes the resistance of the coil, and $\lambda = L(z) \cdot i(t)$ denotes the flux linkage.

In this article, only the mechanical kinetics model and the electromagnetic force model are considered in the magnetic levitation system. Although the proposed model is slightly different from the real one, for overlooking the effect of inductance, the proposed model is simplified and it is easy for controller design.

2.2 Linearized model of the magnetic levitation system

Equation (4) can be rewritten by the Taylor series expansion at the nominal operating point when the error between the variation and nominal point is very small

$$F(i,z) = F(i_0,z_0) + K_i(i-i_0) + K_z(z-z_0) \tag{6}$$

$$K_i = \left.\frac{\partial F(i,z)}{\partial i}\right|_{i=i_0,\quad z=z_0}$$

$$K_z = \left.\frac{\partial F(i,z)}{\partial z}\right|_{i=i_0,\quad z=z_0}$$

where z_0 is the desired air gap distance and i_0 is the corresponding current with the stability of the magnetic levitation system.

When the magnetic levitation system is stable, the electromagnetic force equals to the gravity of the steel ball

$$F(i_0,z_0) + mg = 0 \tag{7}$$

Then, the following equation can be conducted from equations (1), (4), (6), and (7)

$$\frac{\mathrm{d}^2 z}{\mathrm{d}t^2} = -\frac{2g}{i_0}i + \frac{2g}{z_0+p}z + \frac{2gp}{z_0+p} \tag{8}$$

2.3 Model of the controlled system

In this controlled system, the terminal voltage on the electromagnet is defined as the input variation of the system, and the photo-voltage from the position sensor is defined as the output variation of the system.

The current passes through the power amplifier to produce the input voltage. The power amplifier is approximately a proportional amplifier since the response of the circuit is very quick. Hence, the mathematic function of the input voltage and current can be written as

$$u_{\mathrm{in}} = K_{\mathrm{in}} i \tag{9}$$

where K_{in} is a constant value decided by the circuit.

The output voltage of the position sensor can be experimentally measured at a different air gap distance. The collated data are least squares fitted to determine the function between the output voltage and the air gap distance. Figure 3 shows the static

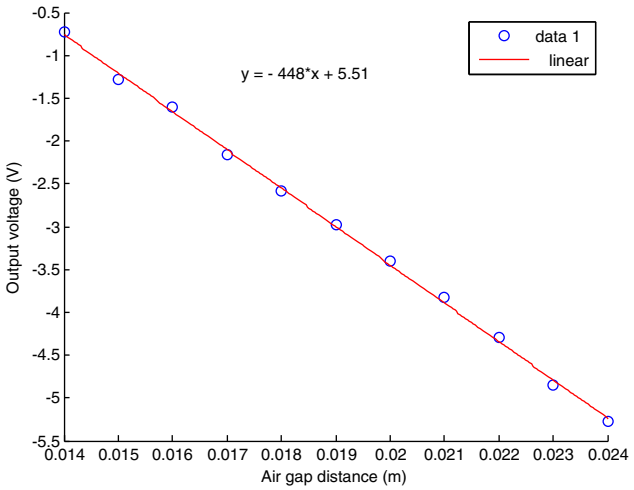

Fig. 3 Fitted static state characteristic curve of the output voltage

state characteristic curve of the output voltage, and the mathematical function of the output voltage and the air gap distance can be represented as

$$u_{\text{out}} = K_{\text{out}}(z + z_{\text{out}}) \tag{10}$$

where K_{out} and z_{out} are constant values determined by the least squares fit.

Combining equations (8) to (10) offers

$$\frac{\mathrm{d}^2 u_{\text{out}}}{\mathrm{d}t^2} + a u_{\text{out}} + l = b u_{\text{in}} \tag{11}$$

$$a = -\frac{2g}{z_0 + p}$$

$$b = -\frac{2gK_{\text{out}}}{i_0 K_{\text{in}}}$$

$$l = \frac{2gK_{\text{out}}}{z_0 + p}(z_{\text{out}} - p)$$

The controlled system is a second-order time-invariant system from the above equation, and it is an unstable system in open loop. Furthermore, the simplified and linearized model of the controlled system is different from the actual system in some degree. To guarantee a satisfied closed-loop performance, therefore, a robust yet effective controller is necessary for this system.

The specifications and system parameters of the proposed magnetic levitation system are listed in Table 1.

3 THE SLIDING MODE CONTROLLER

An SMC is proposed for this magnetic levitation system. The state–space equations and the SMC method are depicted as follows.

Table 1 Specifications and system parameters

Mass of the steel ball	0.11 kg
Gravitational acceleration	9.81 m/s^2
Reference air gap distance at steady state	0.0235 m
Reference current at steady state	0.92 A
L_0	0.575 H
P	0.003 15 m
K_{in}	5.893
K_{out}	−448
A	−736.2
B	1621.3
L	5095.8

3.1 State–space equations

Figure 4 shows the control structure of the magnetic levitation system, where r is the reference input, y is the output, e is the error between r and y, and $e = r - y$, u is the control law, f is the outside disturbance, and it satisfies

$$|bf(t)| \leqslant \varepsilon \tag{12}$$

where ε is a constant parameter and $\varepsilon > 0$.

The differential equation of the system shown in Fig. 4 can be conducted from (11)

$$\frac{\mathrm{d}^2}{\mathrm{d}t^2} y(t) + a y(t) + l = b[u(t) + f(t)] \tag{13}$$

The system state–space equations are as follows by adopting error e as the state variation; suppose $x_1 = e$, then

$$\sum : \begin{cases} \dfrac{\mathrm{d}x_1(t)}{\mathrm{d}t} = x_2(t) \\ \dfrac{\mathrm{d}x_2(t)}{\mathrm{d}t} = -a x_1(t) - b u(t) + F(t) \end{cases} \tag{14}$$

where

$$F(t) = \frac{\mathrm{d}^2}{\mathrm{d}t^2} r(t) + a r(t) + l - b f(t) \tag{15}$$

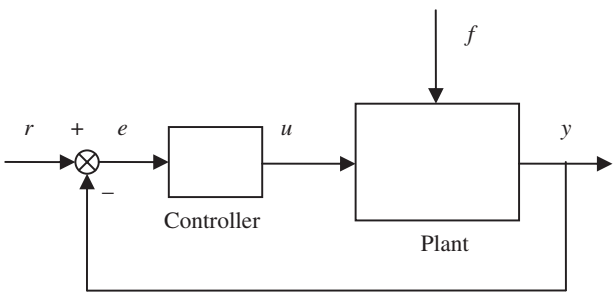

Fig. 4 Control structure of the magnetic levitation system

3.2 Sliding mode control

An SMC is adopted for the magnetic levitation system. First, the sliding surface is chosen. Second, a sliding control law is designed to force the system state trajectories towards the sliding surface and stay on it in a small vicinity bound.

3.2.1 Sliding surface

In a second-order time-invariant system, the sliding surface is a switching line in the phase space. This switching line can be represented by

$$S = cx_1 + x_2 \tag{16}$$

where $c > 0$ is a constant parameter. Therefore, its differential can be

$$\dot{S} = c\dot{x}_1 + \dot{x}_2 \tag{17}$$

3.2.2 Sliding control law

Designing the sliding control law as (18)

$$u = \frac{1}{b}\left(-ax_1 + cx_2 + \frac{\mathrm{d}^2}{\mathrm{d}t^2}r + ar + l + \varepsilon\,\mathrm{sat}(S) + \eta S\right) \tag{18}$$

where η is a constant parameter, $\eta > 0$, and $\mathrm{sat}(S)$ is the saturation function

$$\mathrm{sat}(S) = \begin{cases} 1, & S > \Delta \\ S/\Delta, & |S| \leqslant \Delta \\ -1, & S < -\Delta \end{cases} \tag{19}$$

where Δ denotes a small vicinity of the origin to define the boundary layer, $0 < \Delta < 1$.

The saturation function can convert the discontinuous control into a continuous control. The system state trajectories are bounded in a small vicinity of the switching line $S = 0$, in place of the exactly ideal mode. Since the switching action is replaced by a continuous approximation, the chattering problem can be undermined.

3.2.3 Stability analysis

Employing the positive definite Lyapunov function candidate

$$V = \frac{1}{2}S^2 \tag{20}$$

Combining (14), (15), and (18)

$$\dot{x}_2 = -cx_2 - \varepsilon\,\mathrm{sat}(S) - \eta S - bf \tag{21}$$

Substituting (14) and (21) into (17)

$$\dot{S} = -\varepsilon\,\mathrm{sat}(S) - \eta S - bf \tag{22}$$

Hence,

$$\dot{V} = S\dot{S} = -\varepsilon\,\mathrm{sat}(S)S - \eta S^2 - bfS \tag{23}$$

Since the system behaviour is not determined within the small vicinity, the system will be stable if the phase trajectory can converge into the small vicinity. For this purpose, the saturation function can be replaced by the sign function; therefore

$$\begin{aligned} \dot{V} = S\dot{S} &= -\varepsilon|S| - \eta S^2 - bfS \\ &\leqslant -\varepsilon|S| - \eta S^2 + |bf||S| \\ &\leqslant -\eta S^2 - (\varepsilon - |bf|)|S| \leqslant 0 \end{aligned} \tag{24}$$

This verifies that the system is stable.

3.2.4 System characteristics analysis

It can be calculated from (22) that

$$\begin{cases} S = p_1\,\mathrm{e}^{-\eta t} - \dfrac{\varepsilon\,\mathrm{sign}(S) + bf}{\eta}, & S < \Delta, S > \Delta \\ S = p_2\,\mathrm{e}^{-((\varepsilon/\Delta)+\eta)t} - \dfrac{bf\Delta}{\varepsilon + \eta\Delta}, & |S| \leqslant \Delta \end{cases} \tag{25}$$

where p_1 and p_2 are constant parameters.

Combining (21) and (25) gives

$$\begin{cases} \dot{x}_2 = -cx_2 - \eta p_1\,\mathrm{e}^{-\eta t}, & S < \Delta, S > \Delta \\ \dot{x}_2 = -cx_2 - \left(\dfrac{\varepsilon}{\Delta} + \eta\right) p_1\,\mathrm{e}^{-((\varepsilon/\Delta)+\eta)t}, & |S| \leqslant \Delta \end{cases} \tag{26}$$

$$\begin{cases} x_2 = p_3\,\mathrm{e}^{-ct} + \dfrac{\eta p_1}{\eta - c}\,\mathrm{e}^{-\eta t}, & S < \Delta, S > \Delta \\ x_2 = p_4\,\mathrm{e}^{-ct} + \dfrac{[(\varepsilon/\Delta) + \eta]p_2}{(\varepsilon/\Delta) + \eta - c}\,\mathrm{e}^{-((\varepsilon/\Delta)+\eta)t}, \\ \qquad |S| \leqslant \Delta \end{cases} \tag{27}$$

where p_3 and p_4 are constant parameters.

From equations (16) and (26), the following are obtained

$$\begin{cases} x_1 = -\dfrac{p_1}{\eta - c}\,\mathrm{e}^{-\eta t} - \dfrac{p_3}{c}\,\mathrm{e}^{-ct} \\ \qquad -\dfrac{\varepsilon\,\mathrm{sign}(s) + bf}{\eta}, \quad S < \Delta,\ S > \Delta \\ x_1 = -\dfrac{p_2}{(\varepsilon/\Delta) + \eta - c}\,\mathrm{e}^{-((\varepsilon/\Delta)+\eta)t} - \dfrac{p_4}{c}\,\mathrm{e}^{-ct} \\ \qquad -\dfrac{bf}{c[(\varepsilon/\Delta) + \eta]}, \quad |S| \leqslant \Delta \end{cases} \tag{28}$$

From the above equations, some conclusions can be drawn:

The system dynamic characteristic is decided by η and c before the phase trajectory converges within the small vicinity; the system dynamic characteristic mainly follows ε and Δ within the small vicinity because ε/Δ is far larger than η and c.

Following are the system steady characteristics in the ideal condition

$$\lim_{t\to\infty} S = -\frac{bf\Delta}{\varepsilon+\eta\Delta}$$
$$\lim_{t\to\infty} x_2 = 0$$
$$\lim_{t\to\infty} x_1 = -\frac{bf\Delta}{c(\varepsilon+\eta\Delta)}$$

Although the system characteristics seem satisfying, the system performance could be weakened by the external disturbance, which does not allow intriguing results to be obtained. In this case, the steady error will not tend towards zero if the system does not allow high gain. On the other hand, if the system gain ε/Δ is high, the switching frequency will be high following the sliding surface, which can cause the chattering problem, as discussed earlier. According to (12), the value of ε cannot be small discretionarily; hence, the dynamics characteristics of the system will be debased. Therefore, a novel control law is needed to improve the system performance.

3.3 The improved sliding control law

An asymptotic observer is designed to estimate the unknown disturbance. Then, the estimated disturbance is included in the novel control law in order to undermine the impact of the disturbance. Figure 5 shows the new control structure of the magnetic levitation system including the observer.

3.3.1 The DO

Construct an intermediate variable

$$h = f + K_o x_2 \tag{29}$$

where K_o is a constant observer gain. On the basis of the assumption that the disturbance f is a slow variation system, it is reasonable to impose $\dot{f} = 0$; then

$$\begin{aligned}\dot{h} &= K_o\dot{x}_2 = K_o\left(-ax_1 - bu + \frac{d^2r}{dt^2} + ar + l - bf\right)\\ &= K_o\left(-ax_1 - bu + \frac{d^2r}{dt^2} + ar + l - bh + bK_o x_2\right)\end{aligned} \tag{30}$$

Design an observer for the intermediate variable h as

$$\dot{\hat{h}} = K_o\left(-ax_1 - bu + \frac{d^2r}{dt^2} + ar + l - b\hat{h} + bK_o x_2\right) \tag{31}$$

where $\hat{h}$ denotes the estimated h.

The mismatch between equations (30) and (31) is given as

$$\dot{\tilde{h}} = \dot{\hat{h}} - \dot{h} = -bK_o(\hat{h} - h) = -bK_o\tilde{h} \tag{32}$$

where $\tilde{h}$ denotes the error between the estimated h and the real h. Equation (31) reveals that $\tilde{h}$ tends to zero exponentially and the convergent rate varies with the choice of observer gain K_o.

The disturbance f can be estimated as

$$\hat{f} = \hat{h} - K_o x_2 \tag{33}$$

where $\hat{f}$ denotes the estimated f.

Combination of (29) and (33) gives

$$\tilde{f} = \hat{f} - f = \hat{h} - h = \tilde{h} \tag{34}$$

where $\tilde{f}$ denotes the error between the estimated f and the real f.

As a result, $\hat{f}$ will converge to f asymptotically, and this estimation can be used to design the novel control law.

3.3.2 The novel sliding control law

The updated control law is the following equation

$$\begin{aligned}u = \frac{1}{b}\Bigg(&-ax_1 + cx_2 + \frac{d^2}{dt^2}r + ar + l\\ &+ \varepsilon\,\mathrm{sat}(S) + \eta S - b\hat{f}\Bigg)\end{aligned} \tag{35}$$

The differential of $\hat{f}$can be obtained by combining (31) with (33) and (35)

$$\begin{aligned}\dot{\hat{f}} &= \dot{\hat{h}} - K_o\dot{x}_2\\ &= K_o\left(-ax_1 - bu + \frac{d^2r}{dt^2} + ar + l - b\hat{h} + bK_o x_2\right)\\ &\quad - K_o\dot{x}_2\\ &= -K_o(cx_2 + \dot{x}_2 + \varepsilon\mathrm{sat}(S) + \eta S)\end{aligned} \tag{36}$$

The estimated f can be calculated from (36).

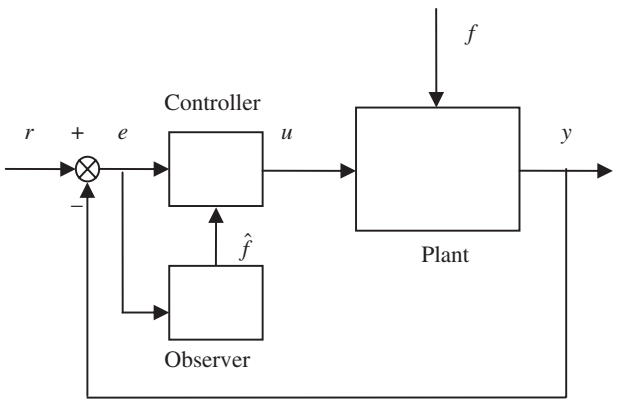

Fig. 5 The new control structure of the magnetic levitation system

Employing the positive definite Lyapunov function candidate

$$V = V_1 + V_2, \quad V_1 = \frac{1}{2}\tilde{f}^2, \quad V_2 = \frac{1}{2}S^2$$
$$\dot{V}_1 = \tilde{f}\dot{\tilde{f}} = \tilde{f}(\dot{\hat{f}} - \dot{f}) = \tilde{f}\dot{\hat{f}}$$
$$= \tilde{f}(\dot{\hat{h}} - K_o\dot{x}_2) = \tilde{f}(-bK_o\tilde{h}) = -bK_o\tilde{f}^2 \leqslant 0$$
$$\dot{V}_2 = S\dot{S} = S(cx_2 + \dot{x}_2) = S(-\varepsilon \mathrm{sat}(S) - \eta S - b\tilde{f}) \tag{37}$$

Like the above analysis, the system behaviour is not determined within the small vicinity, and the saturation function can be replaced by the sign function; therefore

$$\dot{V}_2 = -\varepsilon|S| - \eta S^2 - b\tilde{f}S \leqslant -\eta S^2 - (\varepsilon - |b\tilde{f}|)|S| \leqslant 0 \tag{38}$$

under the assumption of $|b\tilde{f}| \leqslant \varepsilon$.

Hence, $\dot{V} \leqslant 0$, and the system is stable.

Compared to the previous control law, the new one can lower the ε apparently through replacing $|bf|$ by $|b\tilde{f}|$. This modification can ameliorate the system dynamic performance.

4 SIMULATION RESULTS

The proposed system is simulated by using Matlab Simulink. A constant value disturbance and a sinusoidal variation value disturbance are both adopted in the simulation, and the disturbance will not be triggered until the simulation time comes to 1 s. Figure 6 depicts the comparison simulation results of voltage response curves between an SMC without a DO and an SMC with a DO; the SMC without a DO is based on the condition that $r = 5$ V, $c = 20$, $\varepsilon = 2300$, $\eta = 15$, $\Delta = 0.01$, $f = 1$ kg, and the SMC with a DO is based on condition that $r = 5$ V, $c = 20$, $\varepsilon = 0.5$, $\eta = 15$, $\Delta = 0.01$, $K_o = 0.5$, $f = 1$ kg. Figure 9 also represents comparison simulation results of voltage response curves between the SMC without a DO and the SMC with a DO; the only difference from Fig. 6 is that the disturbance is $f = \sin(2\pi t)$ kg. Figures 7 and 10 depict the comparison simulation results of the control law between the SMC without a DO and the SMC with a DO when the disturbance is $f = 1$ kg and $f = \sin(2\pi t)$ kg, respectively. Figures 8 and 11 show the estimated disturbances according to $f = 1$ kg and $f = \sin(2\pi t)$ kg separately. The fixed sample time is $T = 0.003$ s.

As shown in Fig. 6, before the DO is adopted, there is static error between the response and the reference voltage when the constant value disturbance is added into the system; after the DO is employed, there is almost no static error. Besides, in the light of Fig. 7, it can be seen that there is a bit high oscillation in the

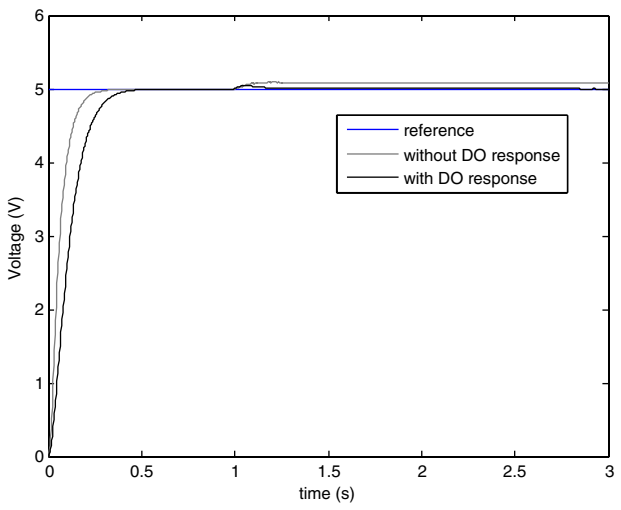

Fig. 6 Voltage response curve ($f = 1$ kg)

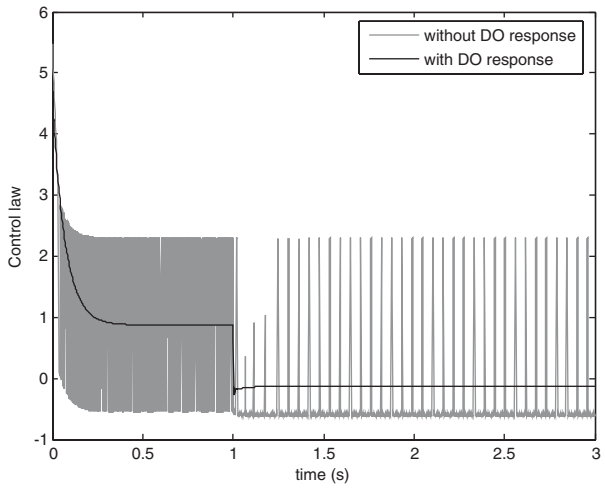

Fig. 7 Control law ($f = 1$ kg)

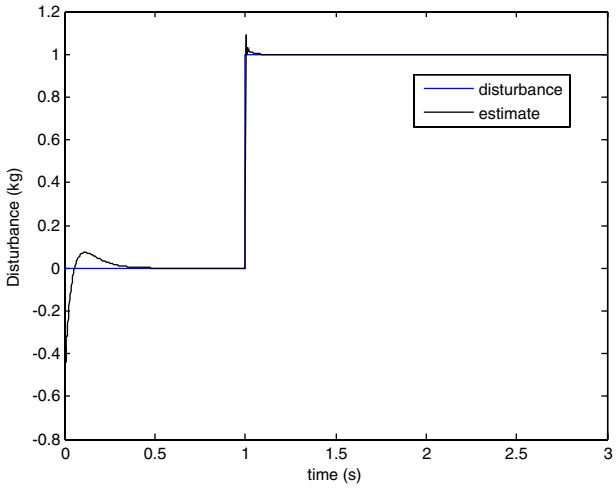

Fig. 8 Estimated disturbance curve with the DO ($f = 1$ kg)

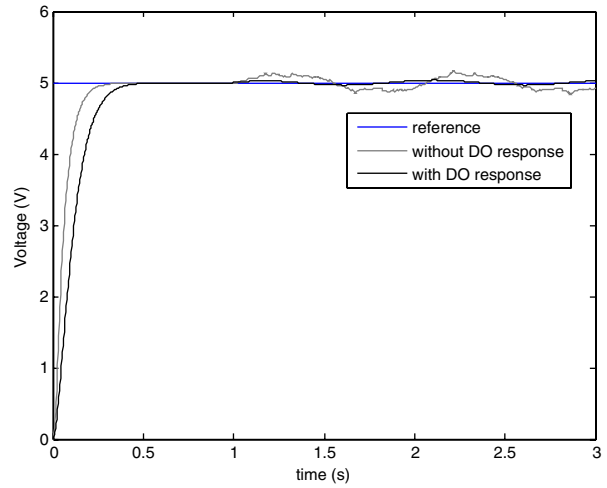

Fig. 9 Voltage response curve ($f = \sin(2\pi t)$ kg)

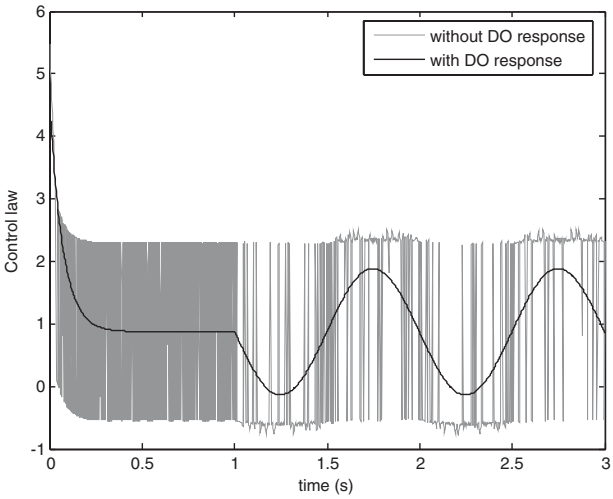

Fig. 10 Control law ($f = \sin(2\pi t)$ kg)

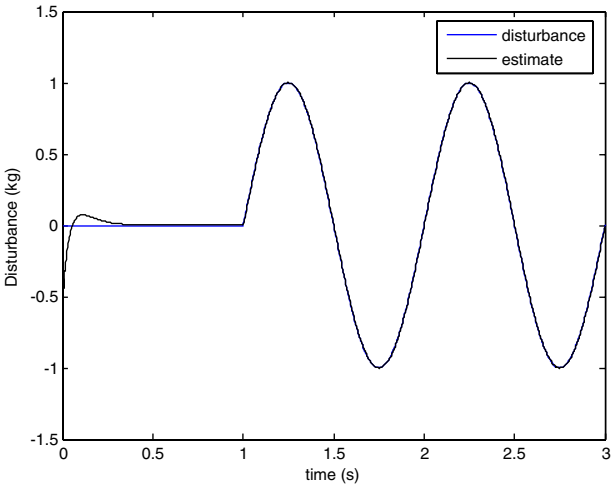

Fig. 11 Estimated disturbance curve with the DO ($f = \sin(2\pi t)$ kg)

control law curve without the DO; the reason for this is that the dynamic switching is too fast for the high gain ε, while the control law curve is smooth with the DO. The result of Fig. 8 shows that the estimated disturbance matches the reference disturbance after a short interim. The findings of these figures show that the system performances are sparklingly promoted when the DO is used. The same conclusions can be drawn from the results of Figs 9–11 when the disturbance is a sinusoidal variation value. These results are identical with the control algorithms of the above section.

5 EXPERIMENTAL RESULTS

Experiments are also carried out to verify the control algorithms. The control algorithms are developed under the Matlab/Simulink environment. The real-time implementation of the magnetic levitation system is executed with the Real Time Workshop (RTW) of Matlab. One data capture and processing card, plugged into a peripheral component interconnect (PCI) bus of the host AMD Athlon XP 1223 MHz computer, is a 16 digital I/O channels and 12 bit A/D converter card.

After the power of the magnetic levitation system is switched on and the control software Matlab/Simulink is running, the controlled steel ball is put into the electromagnetic field in about 2 s. When the steel ball is levitated stably, another steel ball of 0.05 kg, used as the disturbance, is added to the electromagnetic field in around 17 s.

Figures 12(a) and 13(a) represent the experimental results of the SMC without the DO on the condition that $u_{\text{in}} = -5$V, $c = 60$, $\varepsilon = 100$, $\eta = 18$, and $\Delta = 0.01$. Figures 12(b) and 13(b) represent experimental results of the SMC with the DO when the corresponding

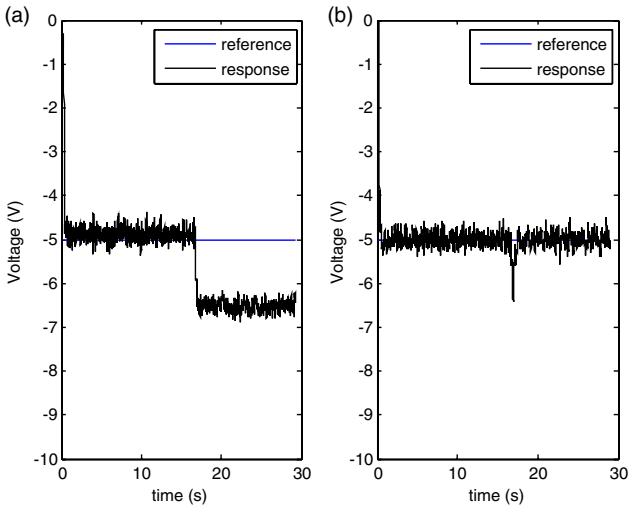

Fig. 12 Voltage response curve ($r = -5$V): (a) SMC without DO and (b) SMC with DO

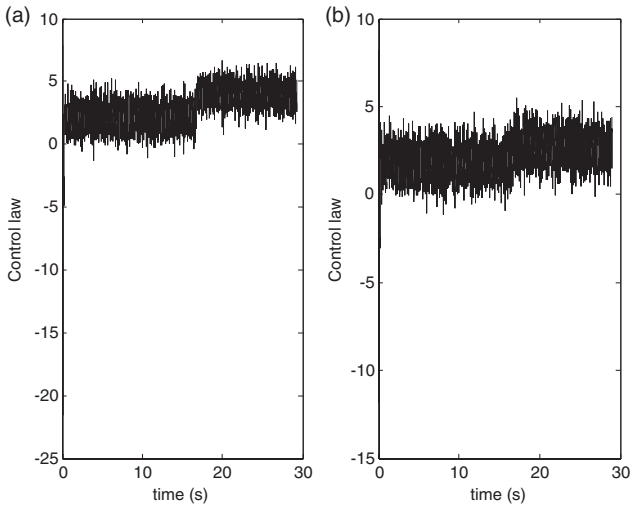

Fig. 13 Control law ($r = -5$ V): (a) SMC without DO and (b) SMC with DO

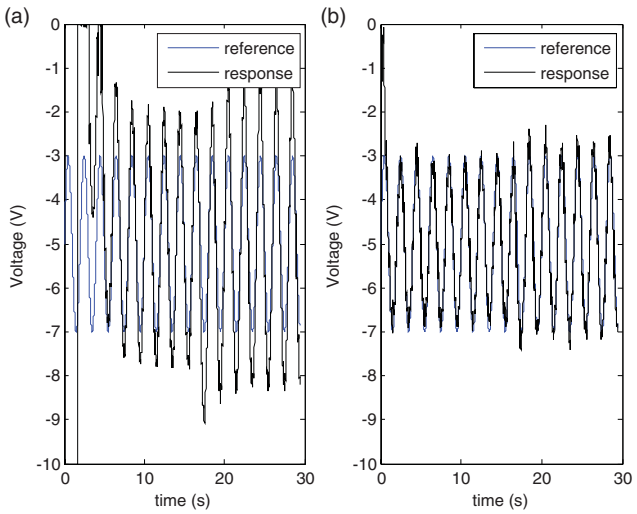

Fig. 15 Voltage response curve ($r = -5 + 2\sin(\pi t)$ V): (a) PID and (b) SMC with DO

parameters are $u_{in} = -5$ V, $c = 8$, $\varepsilon = 0.05$, $\eta = 5$, $K_o = 0.04$, and $\Delta = 0.01$. The fixed sample time for both is $T = 0.003$ s.

Furthermore, the magnetic levitation system performance of an SMC with a DO and that of the traditional PID control are compared when the input voltage is both a constant value and a sinusoidal variation value.

Figure 14(a) shows the experimental result of the traditional PID control with $u_{in} = -5$. The proportional gain, the integral gain, and the derivative gain are $K_p = 1.4$, $K_i = 0.0018$, and $K_d = 12$. The PID gains are selected by trial and error so as to obtain a satisfying system performance because it is difficult to calculate the PID gains for the non-linearity of the magnetic levitation system. Figure 14(b) represents the experimental result of the SMC with the DO when the corresponding parameters are $u_{in} = -5$ V, $c = 8$,

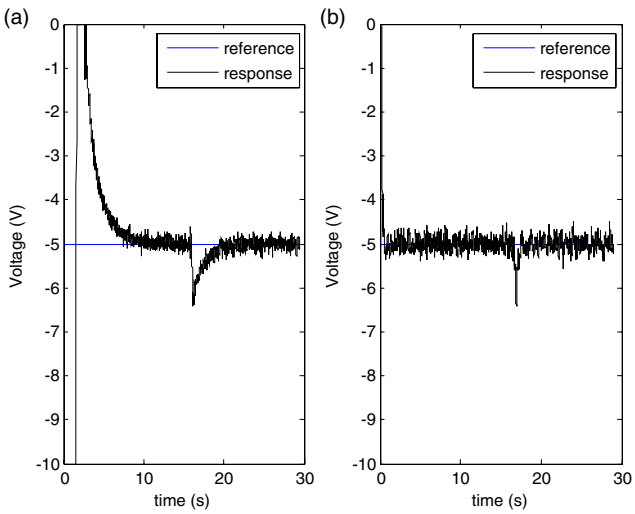

Fig. 14 Voltage response curve ($r = -5$V): (a) PID and (b) SMC with DO

$\varepsilon = 0.05$, $\eta = 5$, $K_o = 0.04$, and $\Delta = 0.01$. Figure 15(a) shows the experimental result of the traditional PID control when the input voltage is a sinusoidal variation value $u_{in} = -5 + 2\sin(\pi t)$, and the PID gains are the same as those in Fig. 14(a) (when $u_{in} = -5$). Figure 15(b) shows the experimental result of the SMC with DO when the input voltage is also sinusoidal variation value $u_{in} = -5 + 2\sin(\pi t)$, and system parameters are the same as those in Fig. 14(b) (when $u_{in} = -5$).

As shown in Fig. 12(a), before adopting the DO, although it can reach a different steady state rapidly when the disturbance steel ball is added to the system, the output voltage deviates from the command. After employing the DO, the response voltage can track the command quickly when there is disturbance in the system. There is no steady error regardless of disturbance when the SMC with DO is used. Figure 13 shows that the control laws switch fast on the two control conditions, the possible reason being that the LED light is sensitive to the environment; this uncertainty will result in the continuous change of the output voltage, and the magnetic levitation system is a highly non-linear system, the control law is correlative to the output voltage.

Comparing Figs 14(a) and (b) when the command voltage is a constant $r = -5$ V, it can be shown that the system can be stable without a steady error either of the proposed sliding mode controller with DO or of the PID controller, and the system dynamic characteristic of the sliding mode controller with DO is a little bit better than that of the PID controller. When the command value is modified to a sinusoidal variation range $r = -5 + 2\sin(\pi t)$, the comparison results are impressed from Figs 15(a) and (b). When using the PID controller, although the response voltage tries to follow the command, there is obvious delay in the trace, and

the system performance is deteriorated when the disturbance ball is put into the system. In contrast, when applying the sliding mode controller with DO, the response voltage curve can track the command very well, and the system performance keeps well regardless of disturbance. It can be concluded that the system performance of the SMC with DO is much better than that of the PID controller, and the SMC with DO is very robust against the disturbance.

The experimental results show that the magnetic levitation system can be stable with either the sliding mode controller without DO or with DO, and the steady error because of the disturbance in the controller without DO is eliminated in the controller with DO, which validate the effectiveness of the proposed SMC with DO. In addition, experimental results reveal that performance of the SMC with DO is superior to that of the traditional PID controller.

6 CONCLUSIONS

In this article, a magnetic levitation system based on SMC is investigated. The model of the magnetic levitation system is constructed, and a sliding mode controller is proposed for this system. The stability and system characteristics of the controller are both analysed. Although the system in this sliding mode controller is stable regardless of disturbance, static error exists when there is disturbance. The static error can be reduced by high system gains, but the dynamic characteristic becomes worse.

An effective DO for SMC is designed so as to withdraw the effects of disturbances. When the unknown disturbance is added to the system, a simple but effective observer is employed to estimate the disturbance. In consequence, the system state trajectory performances are significantly improved, and it is robust against external disturbances. Both the simulation results and experimental results agree with the control algorithms and prove the feasibility of the proposed controllers. Furthermore, the SMC with DO is compared with the traditional PID controller, and the experimental results show that the SMC with DO has overwhelming majority in this non-linear magnetic levitation system, especially when the command signal varies within a wide range.

ACKNOWLEDGEMENT

The authors would like to thank the University Grants Council and the Hong Kong Polytechnic University for the support of this project through the project codes PolyU 5141/05E and G-YX2Q, respectively.

REFERENCES

1 **Hurley, W. G.** and **Wolfle, W. H.** Electromagnetic design of a magnetic suspension system. *IEEE Trans. Educ.*, 1997, **40**(2), 124–130.

2 **El Hajjaji, A.** and **Ouladsine, M.** Modeling and nonlinear control of magnetic levitation systems. *IEEE Trans. Ind. Electron.*, 2001, **48**(4), 831–837.

3 **Joo, S. J.** and **Seo, J. H.** Design and analysis of the nonlinear feedback linearizing control for an electromagnetic suspension system. *IEEE Trans. Control Syst. Technol.*, 1997, **5**(1), 135–144.

4 **Yang, Z.-J.** and **Tateishi, M.** Adaptive robust nonlinear control of a magnetic levitation system. *Automatica*, 2001, **37**, 1125–1131.

5 **Man, Z. H., Paplinski, A. P.,** and **Wu, H. R.** A robust MIMO terminal sliding mode control scheme for rigid robotic manipulators. *IEEE Trans. Autom. Control*, 1994, **39**(12), 2464–2469.

6 **Fujimoto, Y.** and **Kawamura, A.** Robust servo-system based on two-degree-of-freedom control with sliding mode. *IEEE Trans. Ind. Electron.*, 1995, **42**(3), 272–280.

7 **Park, J.-H., Kim, K.-W.,** and **Yoo, H.-H.** Two-stage sliding mode controller for vibration suppression of a flexible pointing system. *Proc. IMechE, Part C: J. Mechanical Engineering Science*, 2001, **215**(C2), 155–166. DOI: 10.1243/0954406011520580.

8 **Vadim, U., Jurgen, G.,** and **Jing, X. S.** Slidng mode control in electromechanical systems, 1999 (Taylor & Francis Ltd, London).

9 **Fallaha, C., Saad, M., Kanaan, H.,** and **Zhu, W.-H.** Sliding mode nonlinear switching functions for control input transient constraints reduction. In Proceedings of the IEEE ISIE 2006, Montreal, Quebec, Canada, 9–12 July 2006, pp. 284–288.

10 **Yang, Z.-J., Miyazaki, K., Kanae, S.,** and **Wada, K.,** Robust position control of a magnetic levitation system via dynamic surface control technique. *IEEE Trans. Ind. Electron.*, 2004, **51**(1), 26–34.

11 **Hassan, D. M. M.** and **Mohamed, A. M.** Variable structure control of a magnetic levitation system. In Proceedings of the American Control Conference, Arlington, VA, 25–27 June 2001, pp. 3725–3730.

12 **Chiang, H.-K., Chen, C.-A.,** and **Li, M.-Y.** Integral variable-structure grey control for magnetic levitation system. *IEE Proc. Electr. Power Appl.*, 2006, **153**(6), pp. 809–814.

13 **Lin, F.-J., Teng, L.-T.,** and **Shieh, P.-H.** Intelligent sliding-mode control using RBFN for magnetic levitation system. *IEEE Trans. Ind. Electron.*, 2007, **54**(3), 1752–1762.

14 **Woodson, H. H.** and **Melcher, J. R.** *Electromechanical dynamics, Part I: discrete systems*, 1968 (John Wiley, New York).

15 **Wilma, A. O., Eduardo, F. C.,** and **Jerson, B. V.** Digital implementation of a magnetic suspension control system laboratory experiments. *IEEE Trans. Educ.*, 1999, **42**(4), 315–322.

16 **Yang, Z. Y., Gerulf, K. M. P.,** and **Jorgen H. P.** Model-based control of a nonlinear one dimensional magnetic levitation with a permanent-magnet object. In *Automation and robotics* (Ed. J. M. R. Arreguin), 2008, pp. 359–374 (I-Tech Education and Publishing, Austria).